

Role of binding energy and deformation parameters in the spontaneous fission of ^{240}Pu nucleus

Kanishka Sharma,* Ashutosh Kaushik, and Manoj K. Sharma

School of Physics and Materials Science,

Thapar Institute of Engineering and Technology, Patiala - 147004, Punjab, INDIA

Introduction

One of the interesting topics in nuclear dynamics is the exploration of fission mass distribution of nuclei formed either via spontaneous decay or the induced decay. The understanding of these mass distributions gives useful information regarding the nuclear properties and related dynamics, and hence one needs to explore them on the experimental as well as the theoretical front. If we concentrate on the ground state decays of a fissile nucleus, the main components which are responsible for the decay structure and related properties are binding energies and the deformation parameters of the emitting fragments. This is because the temperature and angular momentum effects are not included in the spontaneous decays. The recent data on these binding energies and corresponding deformation parameters of nuclei is available in literature [1, 2]. Using these atomic mass evaluation tables (having binding energy data) and the deformation tables, an attempt has been made to analyze the mass distribution of ^{240}Pu radioactive nucleus. The fission distributions are compared with the ones extracted using old sets of binding energies and deformations [3, 4]. The fission fragments having the highest preformation factor have been identified and the magnitude and structure of preformation probability is observed in order to investigate the difference between the old and new sets of binding energy and deformations used. Finally, the fission half-lives have been calculated using the Preformed Cluster-decay Model (PCM).

Methodology

The preformed cluster model (PCM) [5] allows to define the decay half-life $T_{1/2}$, or the decay constant as $\lambda = \nu_0 P_0 P$ and $T_{1/2} = \frac{\ln 2}{\lambda}$. Here, ν_0 is the assault frequency, P_0 is preformation probability and P is the barrier penetrability calculated within WKB approximation. The structure information of the decaying nucleus contained in P_0 is estimated by solving stationary Schrodinger equation in η -coordinate by using the fragmentation potential defined as:

$$V_R(\eta) = - \sum_{i=1}^2 [B(A_i, Z_i)] + V_C + V_P \quad (1)$$

where V_C and V_P are, respectively, the Coulomb and nuclear proximity potentials for deformed and oriented nuclei.

In PCM, P_0 reads as

$$P_0 = |\psi(\eta)|^2 \sqrt{B_{\eta\eta}} \frac{2}{A_{CN}}. \quad (2)$$

Result and discussion

First of all, we have plotted the fragmentation potential $V(\eta)$ of the ground state parent nucleus ^{240}Pu , illustrated in panel (a) of Fig. 1. The fragmentation potential is calculated by including the quadrupole deformations (β_{2i}) and the cold optimum orientations ($\theta_i^{opt.}$) of the fragments. The two curves in the plot are indicating the potentials using two versions of Binding energy and deformation tables. For binding energies, AME1995 [3] and AME2017 [1] of Audi and Wapstra are used, whereas for deformations, the tables of Moller and Nix [2, 4] are used. Fig. 1(a) shows that the overall magnitude and structure of the emitting fragments is similar while we use the old and new binding energy and deformations data. However, a careful look suggests that the structural differences are seen primarily in two regions, first one lies near $A=50-60$

*Electronic address: sharmakanishka730@gmail.com

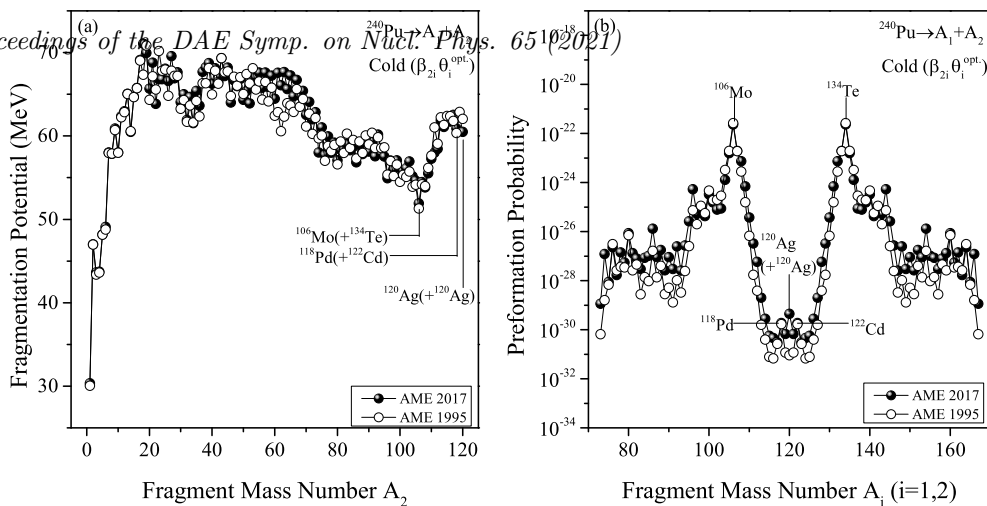


FIG. 1: (a) The fragmentation potential for the decay of parent nucleus ^{240}Pu plotted using two different sets of binding energy and deformation tables for β_2 -cold oriented choice. (b) The corresponding preformation profile of the same nucleus indicating the most probable fragments in the fission regions.

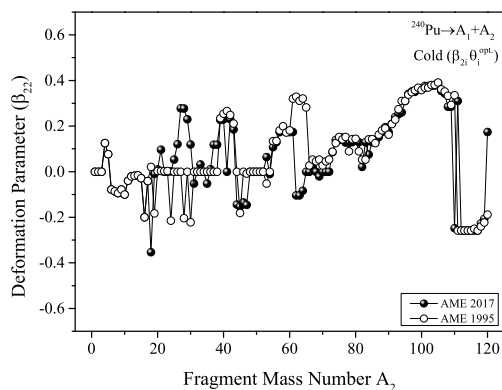


FIG. 2: (a) The deformation parameter with fragment mass number in the decay of parent ^{240}Pu while considering two sets of deformation table.

and the second one is in the fission region. This observation can be clearly described from the preformation probability curves plotted in panel (b) of Fig. 1. Two fission regions are seen in the preformation profile of ^{240}Pu nucleus i.e. asymmetric fission region and symmetric fission region. In symmetric fission region, the most dominating fragment is found to be ^{106}Mo with complementary daughter fragment ^{134}Te (a neutron magic) for both the sets of AME and deformations used. On the other hand, for symmetric fission region, the most probable fragment changes from $^{118}\text{Pd} (+^{122}\text{Cd})$ to $^{120}\text{Ag} (+^{120}\text{Ag})$ when one moves from old set of AME and deformations to the new one. This is primarily due to the significant difference in the deformation param-

eters which are plotted in Fig. 2 for all the probable fragments decaying from ^{240}Pu nucleus. Although the difference in the deformation parameters are seen mainly in the lower mass region, but since PCM follows the collective clusterization approach, the deformations of all the probable emitting fragments affect the overall mass distribution of the decaying fragments. Furthermore, the spontaneous fission half lives have been calculated using PCM and are compared with the experimental data. The PCM calculated $T_{1/2}$ values agree nicely with the experimental numbers while considering the above mentioned symmetric fission fragment as the final emitting fragments. While the asymmetric fission fragment shows deviation in the half life with the experimental data. This result holds good for both the versions of AME and deformations used.

References

- [1] M. Wang, G. Audi *et al*, Chin. Phys. C **41**, 3 (2017).
- [2] P. Moller *et al*, Atomic Data Nucl. Data Tables **109110**, 1204 (2016).
- [3] G. Audi and A. H. Wapstra, Nucl. Phys. A **595**, 409 (1995).
- [4] P. Möller *et al*, At. Nucl. Data Tables **59**, 185 (1995).
- [5] S. Kumar *et al*, Phys. Rev. C **55**, 218 (1997); K. Sharma *et al*, Phys. Rev. C **96**, 054307 (2017).